Spin-phonon coupling in $K_{0.8}Fe_{1.6}Se_2$ and KFe_2Se_2: Inelastic neutron scattering and *ab initio* phonon calculations

R. Mittal,[1] M. K. Gupta,[1] S. L. Chaplot,[1] M. Zbiri,[2] S. Rols,[2] H. Schober,[2,3] Y. Su,[4] Th. Brueckel,[4,5] and T. Wolf[6]

[1]*Solid State Physics Division, Bhabha Atomic Research Centre, Trombay, Mumbai 400 085, India*
[2]*Institut Laue-Langevin, BP 156, 38042 Grenoble Cedex 9, France*
[3]*Université Joseph Fourier, UFR de Physique, 38041, Grenoble Cedex 9, France*
[4]*Juelich Centre for Neutron Science JCNS-FRM II, Forschungszentrum Juelich GmbH, Outstation at FRM II,*
Lichtenbergstr. 1, D-85747 Garching, Germany
[5]*Juelich Centre for Neutron Science JCNS and Peter Gruenberg Institut PGI, JARA-FIT, Forschungszentrum Juelich GmbH,*
52425 Juelich, Germany
[6]*Institut fuer Festkoerperphysik, Karlsruhe Institute of Technology, D-76021 Karlsruhe, Germany*

We report measurements of the temperature dependence of phonon densities of states in $K_{0.8}Fe_{1.6}Se_2$ using inelastic neutron scattering technique. While cooling down to 150 K, a phonon peak splitting $\sim$25 meV is observed and a new peak appears at 31 meV. The measurements support the recent Raman and infrared measurements, indicating a lowering of symmetry of $K_{0.8}Fe_{1.6}Se_2$ upon cooling below 250 K. *Ab initio* phonon calculations have been carried out for $K_{0.8}Fe_{1.6}Se_2$ and KFe_2Se_2. The comparison of the phonon spectra as obtained from the magnetic and nonmagnetic calculations show pronounced differences. We show that in the two calculations, the energy range of the vibrational contribution from both Fe and Se are quite different. We conclude that Fe magnetism is correlated to the phonon dynamics and plays an important role in stabilizing the structure of $K_{0.8}Fe_{1.6}Se_2$, as well as that of KFe_2Se_2. The calculations highlight the presence of low energy optical vibrational modes in $K_{0.8}Fe_{1.6}Se_2$ compared to KFe_2Se_2.

PACS number(s): 74.25.Kc, 78.70.Nx, 63.20.−e

I. INTRODUCTION

The discovery of superconductivity in La-based FeAs ($T_c = 26$ K) compounds has stimulated tremendous interest[1–28] in the field of condensed matter physics. So far, the highest T_c of 56 K has been found in $Gd_{1-x}Th_xOFeAs$.[28] The structural, magnetic, and electronic properties of all the compounds have been extensively investigated[4–6] to understand the mechanism of the superconductivity. The long-range antiferromagnetic order is suppressed with doping in the parent compound. The superconductivity in the compounds appears above a certain doping level. In particular, for all these compounds strong anomalies have been found in the specific heat, resistivity, and magnetic susceptibility in the temperature range of 110–180 K. These anomalies are now known to be prerequisite for superconductivity in FeAs compounds.

Adding to the excitement generated by the discovery of iron-based compounds, the newly discovered alkali-doped iron selenide compounds[13–16] exhibit several unique characters that are noticeably absent in other iron-based superconductors, such as antiferromagnetically ordered insulating phases and extremely high Neel transition temperatures. Neutron-diffraction studies indicate a very large ordered moment and high magnetic transition temperature for these compounds. The T_c of $K_xFe_{2-y}Se_2$ has been reported[13,14] to be ∼31 K under the tetragonal space group $I4/m$. The magnetic phase disappears[15] above $T_N \approx 559$ K followed by the creation of Fe vacancies, which exhibit an ordering transition at 578 K. The refinement of the neutron diffraction pattern shows that the compound can now be chemically expressed as KFe_2Se_2 with a tetragonal symmetry under space group $I4/mmm$. Chemical substitution of K by Rb or Cs also yields a superconductor at a similarly high T_c, as observed

in $Rb_xFe_{2-y}Se_2$[15] and $Cs_xFe_{2-y}Se_2$.[16] Furthermore, the local structure of $K_xFe_{2-y}Se_2$ has been measured[12] by temperature-dependent, polarized, extended x-ray absorption fine structure (EXAFS).

Density functional theory calculations predict systematically weak electron–phonon coupling[7] with a negligible contribution to the superconductivity mechanism in FeAs systems. The role of the phonons for the mechanism of superconductivity is not yet fully established. However, the electron pairing in FeAs compounds is believed to occur beyond the conventional electron–phonon coupling framework. Theoretically, the pairing mechanism is proposed[9,10] to be mediated by exchange of the antiferromagnetic spin fluctuations, which might lead to an interpenetration of electron and hole pockets at the Fermi surface.

Inelastic neutron scattering has been used to study the resonant spin excitations[17–19] in a number of FeAs-based 122, 1111, and 11 compounds. The phonon measurements, as well as the *ab initio* phonon calculations for FeAs compounds, support[25,27] the idea of a possible coupling between spin and lattice degrees of freedom affecting the phonon dynamics. As far as we know, only zone center phonons of $K_{0.8}Fe_{1.6}Se_2$ (also referred to as the $K_2Fe_4Se_5$ phase) have been studied via Raman and infrared spectroscopies.[20–22] In this context, we report results of inelastic neutron scattering measurements of the temperature dependence of phonon spectra over the whole Brillouin zone for $K_{0.8}Fe_{1.6}Se_2$. *Ab initio* phonon calculations are carried out in $K_{0.8}Fe_{1.6}Se_2$ and KFe_2Se_2 for interpretation and analysis of the observed phonon spectra by first lifting and then considering the effect of magnetism. This paper is organized as follows: the details of the experimental technique and lattice dynamical calculations are summarized in Secs. II

and III, respectively. Section IV is dedicated to the presentation and discussion of the results. Conclusions are drawn in Sec. V.

II. EXPERIMENTAL DETAILS

The inelastic neutron scattering experiments on $K_{0.8}Fe_{1.6}Se_2$ were carried out using the IN4C spectrometers at the Institut Laue Langevin, France. The spectrometer is based on the time-of-flight technique and is equipped with a large detector bank covering a range of $\sim 10°$ to $110°$ of scattering angle. Single crystals of $K_xFe_{2-y}Se_2$ were grown by the Bridgman method as previously reported.[29] While we have seen the traces of superconductivity in these crystals with $T_c = 31$ K, the samples are dominated by the insulating $K_{0.8}Fe_{1.6}Se_2$ (also referred to as the $K_2Fe_4Se_5$) phase. A polycrystalline sample of 1 g of $K_{0.8}Fe_{1.6}Se_2$, ground from several small single-crystal pieces, was mounted into a cryostat in the transmission mode, at $45°$ to the incident neutron beam. For these measurements, we have used an incident neutron wavelength of 2.4 Å (14.2 meV) in neutron energy gain setup. The measurements were performed at 300 and 150 K at ambient pressure. In the incoherent one-phonon approximation, the measured scattering function $S(Q, E)$, as observed in the neutron experiments, is related[30] to the phonon density of states $g^{(n)}(E)$ as follows:

$$g^{(n)}(E) = A \left\langle \frac{e^{2W_k(Q)}}{Q^2} \frac{E}{n(E,T) + \frac{1}{2} \pm \frac{1}{2}} S(Q,E) \right\rangle \quad (1)$$

$$g^n(E) = B \sum_k \left\{ \frac{4\pi b_k^2}{m_k} \right\} g_k(E) \quad (2)$$

where the $+$ or $-$ signs correspond to energy loss or gain of the neutrons, respectively, and where $n(E,T) = [\exp(E/k_B T) - 1]^{-1}$. A and B are normalization constants, and b_k, m_k, and $g_k(E)$ are, respectively, the neutron scattering length, mass, and partial density of states of the kth atom in the unit cell. The quantity between $\langle \rangle$ represents the suitable average over all Q values at a given energy, and $2W(Q)$ is the Debye-Waller factor. The weighting factors $\frac{4\pi b_k^2}{m_k}$ for various atoms are 0.050 barns/amu for K, 0.208 barns/amu for Fe, and 0.105 barns/amu for Se. The values of neutron scattering lengths for various atoms can be found from Ref. 31.

III. COMPUTATIONAL DETAILS

The *ab initio* phonon calculations for $K_{0.8}Fe_{1.6}Se_2$ and KFe_2Se_2 are performed in the nonmagnetic phase, as well as by including the effect of magnetic ordering. At room temperature, $K_{0.8}Fe_{1.6}Se_2$ crystallizes in the $I4/m$ space group and contains 44 atoms in a unit cell. The *ab initio* calculations were done using a primitive unit cell of 22 atoms (Table I) with vacancies for K1 and Fe1 at the 2a and 4d Wyckoff sites. In the absence of a fully stoichiometric structure of $K_{0.8}Fe_{1.6}Se_2$, the structure as given in Table I is used for the calculations. As discussed below, the calculated phonon spectra using this structure reproduce correctly the observations. In the nonmagnetic phase, a $2 \times 2 \times 1$ supercell, containing 176 atoms, is used. The magnetic calculations for $K_{0.8}Fe_{1.6}Se_2$ include antiferromagnetic ordering (Fig. 1), as discussed in Ref. 13. The size of the magnetic cell of $K_{0.8}Fe_{1.6}Se_2$
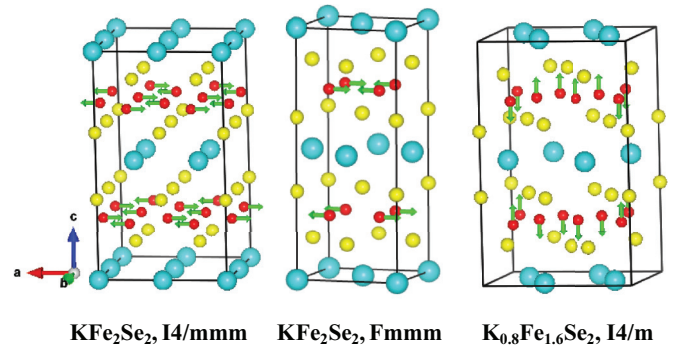

KFe₂Se₂, I4/mmm   **KFe₂Se₂, Fmmm**   **K₀.₈Fe₁.₆Se₂, I4/m**

FIG. 1. (Color online) Magnetic structures of KFe_2Se_2 (tetragonal $I4/mmm$ and orthorhombic $Fmmm$ space groups) and $K_{0.8}Fe_{1.6}Se_2$ (tetragonal space group $I4/m$). The arrow on the Fe atom indicates the magnetic moment direction. A $2 \times 2 \times 1$ super cell is shown for KFe_2Se_2 under the space group $I4/mmm$, while for KFe_2Se_2 under $Fmmm$ and $K_{0.8}Fe_{1.6}Se_2$ under $I4/m$ the unit cell is shown. K, Fe, and Se, are represented by blue, red, and yellow spheres, respectively.

is the same as that of nonmagnetic phase. Total energies and interatomic forces were calculated for the 22 structures resulting from individual displacements of the five symmetry inequivalent atoms along the three Cartesian directions $(\pm x, \pm y, \text{and } \pm z)$.

Upon heating, $K_{0.8}Fe_{1.6}Se_2$ undergoes a nonmagnetic transition at 559 K followed by ordering of Fe vacancies at 578 K. The neutron diffraction data collected at 580 K shows that compound can now be expressed[13] as KFe_2Se_2 under the tetragonal space group $I4/mmm$ with a unit cell containing 10 atoms. KFe_2Se_2 is known to crystallize in the tetragonal space group $I4/mmm$ only. In addition to this phase, calculations are carried out in the orthorhombic space group $Fmmm$, including magnetic ordering. The orthorhombic structure as used in the calculations of KFe_2Se_2 (space group $Fmmm$) is similar to that previously reported for FeAs-based 122 compounds.[5] The supercell approach is adopted (size $2 \times 2 \times 1$), which consists of 40 and 80 atoms in the tetragonal and orthorhombic phase of KFe_2Se_2, respectively. Since KFe_2Se_2 is nonmagnetic, the magnetic calculations are done only for understanding and comparison with the real magnetic case of $K_{0.8}Fe_{1.6}Se_2$. Total energies and interatomic forces were calculated for the 12 (tetragonal $I4/mmm$) and 18 (orthorhombic $Fmmm$) structures resulting from individual displacements of the three symmetry inequivalent atoms along the three Cartesian directions $(\pm x, \pm y, \text{and } \pm z)$.

The phonon calculations for both compounds ($K_{0.8}Fe_{1.6}Se_2$ and KFe_2Se_2) are carried out in the fully relaxed configuration. That is, the lattice constants, as well as the atomic coordinates of the atoms, are fully optimized, with and without the magnetic interactions. In addition, further calculations were performed with a partially relaxed structure, where only the atomic positions were optimized (the lattice parameters were kept at their observed values). Lattice parameters and atomic positions for both systems are given in Table I.

The Vienna *Ab initio* Simulation Package[32,33] software is used for the calculations. The projector-augmented wave method and an energy cutoff of the plane wave of 600 eV were used. The integrations over the Brillouin zone were sampled

TABLE I. Comparison between experimental (Ref. 13) and calculated structural parameters for KFe$_2$Se$_2$ (space group $I4/mmm$) and K$_{0.8}$Fe$_{1.6}$Se$_2$ (space group $I4/m$). The calculations are carried out at 0 K, while the experimental data for K$_{0.8}$Fe$_{1.6}$Se$_2$ and KFe$_2$Se$_2$ are given at 295 and 580 K, respectively. For KFe$_2$Se$_2$ (space group $I4/mmm$), the K, Fe, and Se atoms are located at 2a (0, 0, 0), 4d (0, 0.50, 0.25), and 4e (0, 0, z), respectively. The orthorhombic structure as used in the calculations of KFe$_2$Se$_2$ (space group $Fmmm$) is similar to that previously reported for FeAs-based 122 compounds (Ref. 5). In this phase, the K, Fe, and Se atoms are located at 4a (0, 0, 0), 8f (1/4, 1/4, 1/4), and (0, 0, z), respectively. The experimental structure of K$_{0.8}$Fe$_{1.6}$Se$_2$ (space group $I4/m$) consists (Ref. 13) of atoms at 2a (0, 0, 0) for K1, 8h (x, y, 0) for K2, 4d (0, 1/2, 1/4) for Fe1, 16i (x, y, z) for Fe2, 4e (1/2, 1/2, z) for Se1, and 16i (x, y, z) for Se2, with site occupancies of 1.06, 0.80, 0.059, 1.020, 1, and 1 respectively. In contrast, the *ab initio* calculations were done with vacancies at K and Fe at 2a and 4d Wyckoff sites and atomic positions: 8h (x, y, 0) for K, 16i (x, y, z) for Fe, 4e (1/2, 1/2, z) for Se1, and Se2, 16i (x, y, z).

| | | KFe$_2$Se$_2$ (space group $I4/mmm$) | | | KFe$_2$Se$_2$ (space group $Fmmm$) |
		Experimental	Fully relaxed nonmagnetic	Fully relaxed magnetic	Fully relaxed magnetic
a (Å)		3.94502	3.8382	3.8707	5.5289
b (Å)		3.94502	3.8382	3.8707	5.5075
c (Å)		14.1619	13.4160	13.6984	13.8189
z		0.35444	0.3473	0.3505	0.3537

| | | K$_{0.8}$Fe$_{1.6}$Se$_2$ (space group $I4/m$) | | |
		Experimental	Fully relaxed nonmagnetic	Partially relaxed magnetic	Fully relaxed magnetic
	a (Å)	8.7308	8.6049	8.7308	8.6760
	c (Å)	14.1128	13.3871	14.1128	14.3677
K	x	0.403	0.3705	0.3766	0.3740
	y	0.180	0.1903	0.1856	0.1855
Fe	x	0.1984	0.1941	0.1934	0.1938
	y	0.0918	0.1048	0.0943	0.0942
	z	0.2515	0.2495	0.2485	0.2484
Se1	z	0.1351	0.1500	0.1337	0.1350
Se2	x	0.1147	0.0958	0.1080	0.1081
	y	0.3000	0.3055	0.3024	0.3027
	z	0.1462	0.1604	0.1504	0.1510

on a 4 × 4 × 4 mesh of k-points generated by Monkhorst-Pack method.[34] The exchange-correlation contributions were approached within the generalized gradient approximation framework and described by the Perdew–Burke–Ernzerhof density functional.[35,36] The convergence criteria for the total energy and ionic forces were set to 10^{-8} eV and 10^{-5} eV Å^{-1}, respectively. Phonon spectra for both compounds were extracted using the Phonon software.[37]

IV. RESULTS AND DISCUSSION

A. Temperature dependence of phonon spectra

The phonon spectra for K$_{0.8}$Fe$_{1.6}$Se$_2$ measured at 300 and 150 K using the IN4C spectrometer are shown in Fig. 2. The high-resolution measurements performed with small incident neutron energy of 14.2 meV can be done in the neutron-energy gain mode. At 300 K, the peaks in the phonon spectra are located around 10, 25, and 29 meV. When cooling down, the peak centered at 25 meV splits into two peaks centered at 23.5 and 26.5 meV, in addition to a new peak appearing ~31 meV. Peak splitting and the appearance of a new peak

indicate lowering of the symmetry. Our measurements are consistent with recent temperature-dependent Raman and infrared measurements[21] on the stoichiometrically closely similar compound K$_{0.75}$Fe$_{1.75}$Se$_2$. For the latter and below 250 K, new Raman modes appear ~20.5, 24.9, and 26.2 meV (165, 201, and 211 cm^{-1}, respectively), while the new infrared active modes appear ~12.3, 21.2, and 30.5 meV (99, 171, and
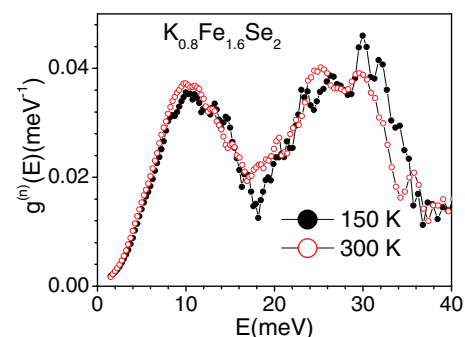

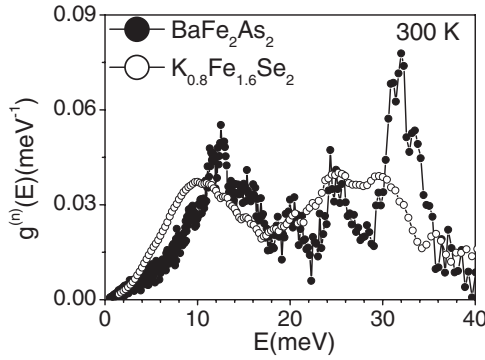FIG. 2. (Color online) The experimental phonon spectra for K$_{0.8}$Fe$_{1.6}$Se$_2$ at 150 and 300 K.

FIG. 3. The experimental phonon spectra for $K_{0.8}Fe_{1.6}Se_2$ and $BaFe_2As_2$ (Ref. [27]) at 300 K.

246 cm^{-1}, respectively). The new modes are nonactive Raman (nonactive infrared) $A_u(E_g)$ or silent B_u within the space group $I4/m$. The authors[30] concluded that $K_{0.75}Fe_{1.75}Se_2$ undergoes a structural phase transition from $I4/m$ to $I4$, accompanied by the loss of inversion symmetry below 250 K. The Fe-Se stretching $\sim$30 meV are found to shift to slightly higher energies at 150 K, as expected from the unit cell volume decrease upon cooling from 300 to 150 K.

Furthermore, other work using Raman spectroscopy[20] shows that the A_g mode at 8.2 meV (66 cm^{-1}) behaves rather anomalously. The intensity of this mode is found to decrease significantly with increase of temperature. Our inelastic neutron scattering measurements indicate (Fig. 1) that the intensity of phonon modes $\sim$9 meV exhibits similar behavior. As these measurements were done in the neutron energy gain mode, no data were collected across the superconducting transition at 31 K. Nevertheless, Raman measurements show[20] that the superconducting transition has little effect on the phonon energies. At T_c, the A_g mode at 180 cm^{-1} exhibits only a jump of $\sim$1 cm^{-1} (0.12 meV).

Figure 3 compares the phonon spectrum of $K_{0.8}Fe_{1.6}Se_2$ with our previously published data on $BaFe_2As_2$.[25,27] The energy range of phonon spectra in both compounds is found to be nearly the same. However, phonon peaks in $K_{0.8}Fe_{1.6}Se_2$ are broader compared to those in $BaFe_2As_2$. There are three well-separated peaks at 20, 25, and 32 meV in the energy range extending from 18 to 35 meV in $BaFe_2As_2$, compared to the broad peaks at 20, 25, and 30 meV in $K_{0.8}Fe_{1.6}Se_2$. This is well supported by EXAFS measurements[12] carried out on $K_{0.8}Fe_{1.6}Se_2$ at the Fe and Se K edges that indicate a large static disorder along the c axis, as well as disorder on the Fe site. Such a structural disorder may result in broadening of the peaks in the phonon spectra, as presently observed. The Fe-Se stretching modes at 30 meV in $K_{0.8}Fe_{1.6}Se_2$ are found to be shifted to slightly lower energies due to the slightly larger Fe-Se bond length of 2.42 Å in $K_{0.8}Fe_{1.6}Se_2$ compared to the Fe-As bond length of 2.4 Å in $BaFe_2As_2$.[4]

B. Effect of magnetic ordering on phonon spectra

The electronic properties of the FeAs-based compounds are known to be sensitively controlled by distortions of the FeAs$_4$ tetrahedra in terms of As-Fe-As bond angle and Fe-As bond length. Earlier, it was shown[28] that the strong interaction

between the As ions in FeAs compounds is controlled by the Fe-spin state. The noninclusion of the Fe magnetic moment in the calculations weakens the Fe-As bonding, which in turn increases the As-As interactions and decreases their repulsive character, leading to the axial collapse along the c axis. Including the iron magnetic moments in the *ab initio* calculations leads to a significant change in the electronic structure, as this is induced by the correct description of the Fe 3d states near the Fermi level. Consequently, this improves the agreement between the calculated and the experimental structural, as well as dynamical, properties.

The calculated magnetic moment for the equilibrium structure is 2.9 μ_B ($I4/m$) for $K_{0.8}Fe_{1.6}Se_2$, while for KFe_2Se_2, the values are 1.8 μ_B ($I4/mmm$) and 2.4 μ_B ($Fmmm$) for calculations carried out under tetragonal and orthorhombic space groups, respectively. The calculated value of the magnetic moment in $K_{0.8}Fe_{1.6}Se_2$ agrees closely with the experimentally refined one[13] of 3.3 μ_B at 11 K. For KFe_2Se_2, calculated values of magnetic moments are close as that obtained from the *ab initio* calculated value[27] of 1.9 μ_B for $BaFe_2As_2$.

The neglect of the spin degrees of freedom in the calculations carried out for $K_{0.8}Fe_{1.6}Se_2$ results in a collapse of the c-lattice parameter value from 14.11 to 13.39 Å. However, by including Fe magnetism, the lattice structure is described correctly (Table I). For the other compound KFe_2Se_2, which is reported to be paramagnetic[13] above 580 K, we find that the optimized structure without any magnetic moment at the Fe sites is collapsed along the c axis, with a value of the axial parameter decreasing from 14.16 to 13.42 Å. Interestingly, by including magnetic ordering on the Fe sites in the $I4/mmm$ space group, the estimated c-lattice parameter value (13.70 Å) is reasonably close to the experimentally refined one. Under the orthorhombic phase ($Fmmm$), the calculated relaxed c-lattice parameter value of KFe_2Se_2 is 13.82 Å. The detailed comparison between the experimental and the calculated structural parameters for both compounds is given in Table I.

The main difference between the magnetic and the nonmagnetic calculations is reflected in terms of phonon modes above 20 meV (Fig. 4). We find that the magnetic lattice dynamical calculations reproduce correctly the experimental data compared to the nonmagnetic case. The good agreement between the experimental data and the magnetic calculations highlights a signature of a magnetostructural correlation, which affects phonon dynamics in $K_{0.8}Fe_{1.6}Se_2$. However, a slight difference between estimations and observations is seen, and it could originate from $K_{0.8}Fe_{1.6}Se_2$ (Ref. [12]) having large static disorder along the c axis, as well as large Fe site disorder, which is not included perfectly in the state of the art *ab initio* phonon calculations. Furthermore, magnetic phonon calculations were done with full and partial (by keeping values of the experimental lattice parameters) structural relaxation. However, the magnetic calculations based on a partially optimized crystal structure seem to offer slightly better agreement with the experimental data. Therefore, in the following, magnetic calculations refer to those carried out with a partially relaxed structure.

The contribution of the various atomic motions to the phonon spectra can be understood from the calculated partial densities of states (Fig. 5). It is found that vibrations of the
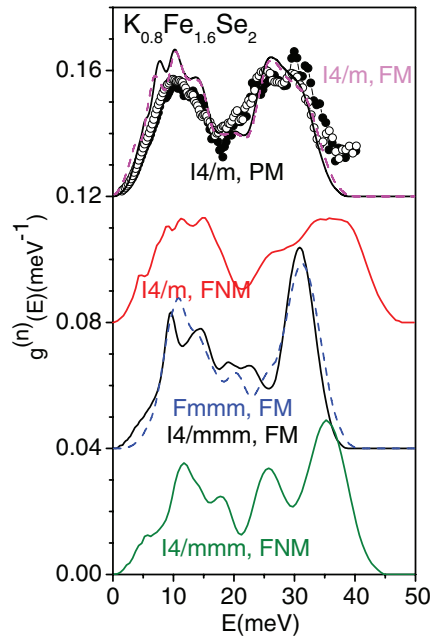
FIG. 4. (Color online) The experimental and calculated phonon spectra for K$_{0.8}$Fe$_{1.6}$Se$_2$ (space group $I4/m$) and KFe$_2$Se$_2$ (space groups $I4/mmm$ and $Fmmm$). The solid and open symbols correspond to the experimental data at 150 and 300 K, respectively. FM, FNM, and PM refer to fully relaxed magnetic, fully relaxed nonmagnetic, and partially relaxed magnetic calculations, respectively.

K atoms dominate mainly the spectra up to 20 meV in both the magnetic and the nonmagnetic calculations. The atomic vibrations due to Fe and Se span the whole energy range. The
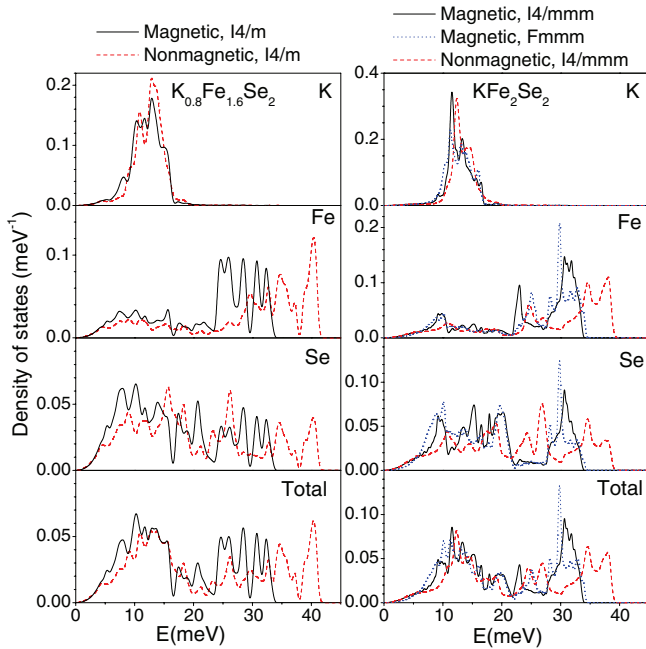

FIG. 5. (Color online) The calculated partial density of states for various atoms and the total phonon density of states for K$_{0.8}$Fe$_{1.6}$Se$_2$ (space group $I4/m$) and KFe$_2$Se$_2$ (space groups $I4/mmm$ and $Fmmm$). For K$_{0.8}$Fe$_{1.6}$Se$_2$, partially relaxed magnetic phonon calculations are shown, while for KFe$_2$Se$_2$, fully relaxed magnetic calculations were done (cf. the text).

FIG. 6. (Color online) The calculated phonon dispersion curves for K$_{0.8}$Fe$_{1.6}$Se$_2$ (space group $I4/m$) and KFe$_2$Se$_2$ (space groups $I4/mmm$ and $Fmmm$). For K$_{0.8}$Fe$_{1.6}$Se$_2$, partially relaxed magnetic phonon calculations are shown, while for KFe$_2$Se$_2$, fully relaxed magnetic calculations were done (cf. the text).
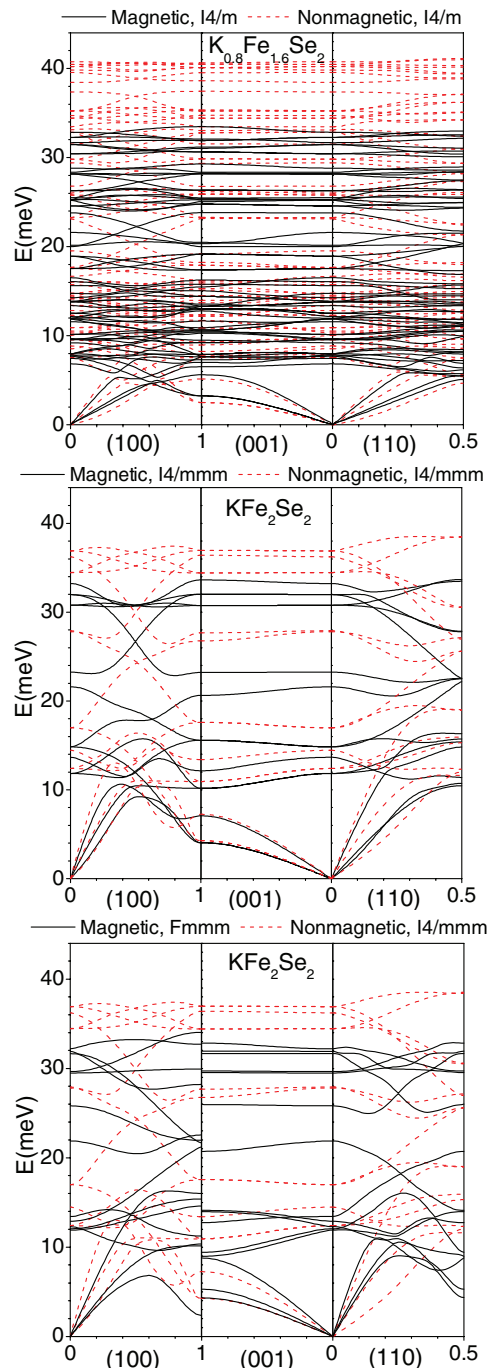
inclusion of magnetic ordering in the calculations significantly softens the Fe and Se vibrations, as shown in Fig. 5. The Fe-Se stretching modes are above 30 meV.

The differences in the partial densities of states (Fig. 5) in both calculations can also be understood from the calculated phonon dispersion relations represented in Fig. 6. All the phonon dispersions have a large number of slightly dispersive branches up to 20 meV, resulting in a broad peak in the low

TABLE II. The calculated zone center optic phonon modes (in reciprocal centimeters) for KFe$_2$Se$_2$ (1 meV = 8.0585 cm^{-1}) in the tetragonal ($I4/mmm$) and orthorhombic ($Fmmm$) space groups.

| | Space group $I4/mmm$ | | Space group $Fmmm$ | |
	Fully relaxed nonmagnetic	Fully relaxed magnetic		Fully relaxed magnetic
A_g	224	174	A_g	176
B_g	225	188	B_{1g}	208
E_g	137	120	B_{2g}, B_{3g}	99, 104
	298	258		257, 255
A_u	117	101	B_{1u}	108
	292	268		260
E_u	100	96	B_{2u}, B_{3u}	97, 96
	277	248		238, 239

TABLE III. The experimental (Ref. 21) and calculated zone center optic phonon modes (in reciprocal centimeters) for K$_{0.8}$Fe$_{1.6}$Se$_2$ (tetragonal space group $I4/m$) (1 meV = 8.0585 cm^{-1}).

	Experimental	Fully relaxed nonmagnetic	Partially relaxed magnetic	Fully relaxed magnetic
A_g	67.6	71	64	62
	81.0	85	78	78
	111.8	110	96	95
	124.8	127	115	114
	135.9	158	133	132
	182.5	209	174	178
	205.3	267	204	203
	242.3	284	229	232
	267.9	317	254	255
B_g	63.1	64	55	53
		83	78	74
	100.6	114	96	97
	103.3	137	126	124
	143.6	188	131	128
	195.3	237	192	191
	216.1	269	206	209
	277.1	324	254	260
E_g		79	64	60
		100	77	77
		115	101	99
		142	112	111
		207	153	152
		240	198	202
		283	212	213
		324	246	249
A_u		71	63	63
		115	98	101
		118	108	105
		210	162	160
		252	203	205
		301	232	236
		307	265	269
B_u		84	60	56
		104	74	73
		121	93	89
		145	119	119
		216	161	160
		280	227	229
		317	256	261
E_u		64	62	56
		87	82	79
		108	96	94
		131	111	110
		187	141	142
		264	204	204
		277	227	228
		320	260	266

energy region of the phonon spectra (Fig. 5). The phonon branches ∼20 meV (Fig. 6) soften by 5–8 meV in the magnetic calculations compared to the nonmagnetic case. The collapse of the c-lattice parameter in the nonmagnetic calculations from 14.11 to 13.39 Å results in a significant change in Fe-Se bond length and in turn overestimates the high energy stretching modes in the nonmagnetic calculations.

Neutron diffraction measurements show that KFe$_2$Se$_2$ stabilizes at ∼578 K and that it is paramagnetic. The primitive cell of KFe$_2$Se$_2$ has only 5 atoms, in comparison to 22 atoms in K$_{0.8}$Fe$_{1.6}$Se$_2$. The increase in symmetry in the high temperature phase results in lowering of a number of phonon branches in the phonon dispersion relation of KFe$_2$Se$_2$ (Fig. 6). The nearly flat optic branches result in sharp features in the density of states (Figs. 4 and 5). Although phonon density of states (Fig. 1) measurements are carried out only for K$_{0.8}$Fe$_{1.6}$Se$_2$, the range of phonon spectra is expected to be the same in both compounds. Again, as far as the energy range of phonon spectra is concerned, it is found that the calculated phonon spectra, including magnetism on the Fe sites, compare well with the experimental data and the other magnetic calculations of K$_{0.8}$Fe$_{1.6}$Se$_2$. The calculated (with and without magnetism) partial density of states for KFe$_2$Se$_2$ (Fig. 5) exhibit the same characteristics as in the case of K$_{0.8}$Fe$_{1.6}$Se$_2$. Our calculations clearly support that although KFe$_2$Se$_2$ is paramagnetic, Fe magnetism is always present, even at temperatures well above the magnetic ordering temperature, and controls the structure, the phonon energies, and probably the superconducting properties of FeSe-based compounds.

The detailed comparison of the phonon spectra calculated including magnetic ordering in the orthorhombic ($Fmmm$) and tetragonal ($I4/mmm$) space groups shows (Figs. 4 and 5) that the calculated B_g and E_g modes at 23.5 and 15 meV (as discussed in Sec. IV C) in the $I4/mmm$ space group are most affected due to the inclusion of the orthorhombic distortion. We find that in the orthorhombic phase ($Fmmm$ space group), the peak in the calculated phonon spectrum 15 meV broadens and there is an enhancement of intensity of peak at 11 meV compared to that in the tetragonal phase ($I4/mmm$ space

group). Furthermore, the two-peak structure in the calculated spectra of $I4/mmm$ space group in the energy range of 18–23 meV (Fig. 4) disappears, and we find a single peak at 20 meV in the orthorhombic space group. The calculated partial density of states (Fig. 5) reflects that all these changes are associated with the change in the partial contribution of Fe and Se atoms. This may be because the difference in the type of
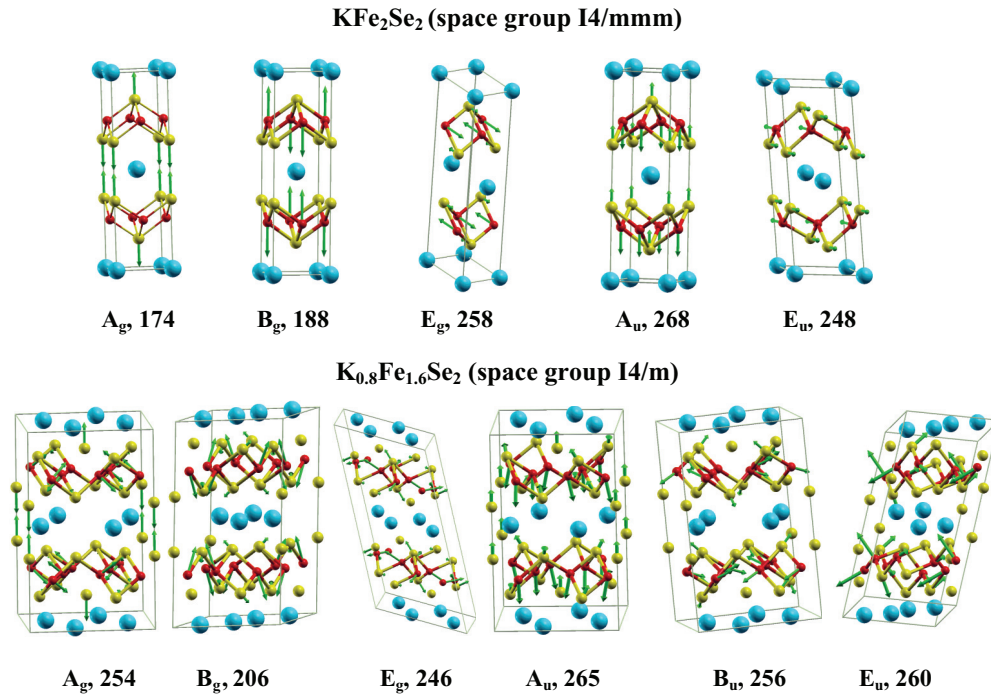
KFe$_2$Se$_2$ (space group I4/mmm)

A$_g$, 174   B$_g$, 188   E$_g$, 258   A$_u$, 268   E$_u$, 248

K$_{0.8}$Fe$_{1.6}$Se$_2$ (space group I4/m)

A$_g$, 254   B$_g$, 206   E$_g$, 246   A$_u$, 265   B$_u$, 256   E$_u$, 260

FIG. 7. (Color online) Polarization vectors of selected zone center modes in KFe$_2$Se$_2$ (space group $I4/mmm$) and K$_{0.8}$Fe$_{1.6}$Se$_2$ (space group $I4/m$), showing exceptionally high softening upon inclusion of magnetic ordering in the phonon calculations. For each mode, the assignment and frequency are indicated in reciprocal centimeter units. The length of the arrows is related to the displacement of the atoms. The absence of an arrow on an atom indicates that the atom is at rest. The number after the mode assignment gives the phonon frequency as calculated from partially relaxed magnetic and fully relaxed magnetic calculations in the tetragonal space groups for K$_{0.8}$Fe$_{1.6}$Se$_2$ and KFe$_2$Se$_2$, respectively. The c axis is vertical, while the a and b axes are in the horizontal plane. K, Fe, and Se, are represented by blue, red, and yellow spheres, respectively (1 meV = 8.0585 cm^{-1}).

magnetic ordering (Fig. 1) in the two calculations would affect the Fe-Se bonding and in turn lead to a change of the phonon frequencies associated with Fe and Se atoms. The comparison of the phonon dispersion relation (Fig. 6) in both space groups shows that significant changes in the phonon branches are in the energy range of 15–25 meV, consistent with the phonon density of states (Figs. 4 and 5).

Recently, *ab initio* phonon dispersion calculations[11] have been reported for KFe$_2$Se$_2$. The authors found that phonon branches ~100–150 cm^{-1} (~12–18 meV) in their nonmagnetic calculations soften by ~50 cm^{-1} (~6 meV) when magnetic interactions are considered while calculating the interatomic force constants for the dynamical matrix. The high energy phonon modes also show slight softening in the magnetic calculations. It is well established that unit cell optimization in the *ab initio* calculations without including spin polarization leads to a collapse of the c-lattice parameter, which in turn results in an overestimation of the energies of the stretching modes. We found that phonon branches ~12–18 meV in nonmagnetic calculations soften by ~4 meV when magnetic interactions are considered in the space group *Fmmm*. Furthermore, the nonmagnetic Fe-Se stretching modes ~35–42 meV soften by ~8 meV when magnetic degrees of freedom are included.

C. Zone center phonon modes

At ambient conditions, K$_{0.8}$Fe$_{1.6}$Se$_2$ crystallizes in the tetragonal structure $I4/m$. The group theoretical

decomposition of the phonon modes at the zone center is given by

$$\Gamma = 9A_g + 8B_g + 8E_g + 9A_u + 7B_u + 10E_u.$$

Similarly, the 15 phonon modes of KFe$_2$Se$_2$ at the zone center within the space groups $I4/mmm$ and $Fmmm$ can be classified as

$$\Gamma = A_g + B_g + 2E_g + 3A_u$$
$$+ 3E_u \text{ (tetragonal space group } I4/mmm)$$

$$\Gamma = A_g + B_{1g} + 2B_{2g} + 2B_{3g} + 3B_{1u} + 3B_{2u}$$
$$+ 3B_{3u} \text{ (orthorhombic space group } Fmmm)$$

The A_g, B_g, and E_g modes are Raman active, while A_u, B_u, and E_u are infrared active. The B_u modes are silent. The calculated zone center modes of KFe$_2$Se$_2$ and K$_{0.8}$Fe$_{1.6}$Se$_2$ are gathered in Tables II and III, respectively. Experimental Raman data[21] as available for K$_{0.8}$Fe$_{1.6}$Se$_2$ are also shown in Table III. The calculations including magnetic ordering compare well with the available experimental Raman data. The high stretching energy modes are found to soften by ~6–8 meV, in agreement with the calculated density of states, as well as phonon dispersion relations (Figs. 4–6). The comparison of zone center modes (Table II) for KFe$_2$Se$_2$ under the space groups $I4/mmm$ and $Fmmm$ show that the orthorhombic distortion splits the doubly degenerate modes into nondegenerate ones. The B_g and E_g modes in the $I4/mmm$
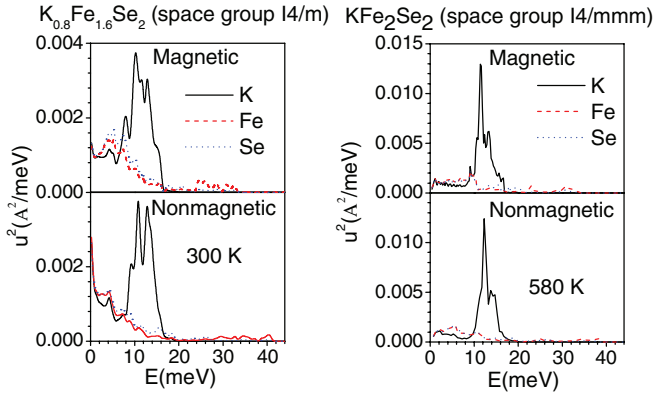
FIG. 8. (Color online) The calculated contribution to the mean squared amplitude of the various atoms arising from phonons of energy E at $T = 300$ and 580 K in $K_{0.8}Fe_{1.6}Se_2$ (space group $I4/m$) and KFe_2Se_2 (space group $I4/mmm$). For $K_{0.8}Fe_{1.6}Se_2$, partially relaxed magnetic phonon calculations are shown, while for KFe_2Se_2, fully relaxed magnetic calculations were done (cf. the text).

space group at 188 and 120 cm^{-1} show maximum shift, as estimated from calculations in the *Fmmm* space group. The B_g mode at 188 cm^{-1} hardens to 208 cm^{-1}, while the E_g mode at 120 cm^{-1} softens and splits at frequencies of 99 and 104 cm^{-1}. For other modes, the splitting or change detected from comparing *Fmmm* and $I4/mmm$ space group calculations is found to be below 10 cm^{-1}. Hereafter, the eigenvectors of some selected modes showing the large softening are plotted in Fig. 7.

The A_g mode at 224 cm^{-1} (27.8 meV) from the nonmagnetic calculations of KFe_2Se_2 (Fig. 7) involves only displacement of Se atoms in the opposite direction along the c axis, whereas K and Fe atoms are at rest. This mode is found to soften by 6 meV in the magnetic calculation. This clearly shows that neglecting magnetic ordering at the Fe sites in the calculations has a crucial influence on the binding in the compound and therefore on the phonon frequencies. When the c axis collapses, this leads to a change of the height (z parameter) of Se atoms, resulting in an overestimation of the phonon energies in the nonmagnetic calculations.

D. Mean squared displacements of various atoms

Figure 8 shows the calculated mean squared displacements of the various atoms, expressed as u^2 and arising from all phonons of energy E within the Brillouin zone. This is relevant to the understanding of the averaged nature of phonons in the

entire Brillouin zone. The calculated phonon densities of states (Fig. 4) were used for these calculations. The structures of $K_{0.8}Fe_{1.6}Se_2$ and KFe_2Se_2 consist of Fe-Se layers, separated by K atoms at $c/2$. Each of the Fe-Se layers has $FeSe_4$ and $SeFe_4$ units.

The calculated u^2 (Fig. 8) shows that for energies of 8–18 and 12–18 meV in KFe_2Se_2 and $K_{0.8}Fe_{1.6}Se_2$, respectively, K atoms have very large vibrational amplitudes in comparison to those of Fe and Se atoms, indicating the weak interaction between K atoms and Fe-Se layers. The Fe and Se atoms in both compounds have nearly the equal amplitude in the entire energy range. The calculated u^2 for K atoms seems not to be sensitive to whether magnetic ordering is considered or not. For higher energies above 18 meV, K atoms do not contribute while u^2 values for Fe and Se atoms are small. Including the magnetic interaction in $K_{0.8}Fe_{1.6}Se_2$ calculations enhances the amplitude of Fe and Se atoms, while it does not affect the calculated u^2 of atoms in KFe_2Se_2, which are nonmagnetic.

V. CONCLUSIONS

We have reported detailed measurements of the temperature dependence of the phonon density of states of $K_{0.8}Fe_{1.6}Se_2$ using the inelastic neutron scattering technique. While cooling down to 150 K, a phonon peak splitting $\sim$25 meV is observed and a new peak appears at 31 meV. This suggests a structural phase transition below 250 K involving symmetry lowering. The phonon spectra of $K_{0.8}Fe_{1.6}Se_2$ have been analyzed based on detailed nonmagnetic, as well as magnetic, *ab initio* lattice dynamical calculations. Furthermore, calculations are performed for the nonmagnetic KFe_2Se_2 under the tetragonal ($I4/mmm$) and orthorhombic (*Fmmm*) space groups. The calculated partial densities of states show that the range of the K vibrations does not affect inclusion of magnetic ordering, while vibrations due to the Fe and Se atoms soften. The comparison of the experimental and the calculated phonon spectra shows that magnetism should be considered in order to correctly describe phonon dynamics. It is found that magnetism due to the unpaired electrons of Fe sites does not vanish upon heating above 578 K, and it controls the structure and phonon energies of FeSe-based compounds, suggesting a spin-phonon coupling.

[1] Y. Kamihara, T. Watanabe, M. Hirano, and H. Hosono, J. Am. Chem. Soc. **130**, 3296 (2008).

[2] H. Takahashi, K. Igawa, K. Arii, Y. Kamihara, M. Hirano, and H. Hosono, Nature **453**, 376 (2008).

[3] C. Wang, L. Li, S. Chi, Z. Zhu, Z. Ren, Y. Li, Y. Wang, X. Lin, Y. Luo, S. Jiang, X. Xu, G. Cao, and Z. Xu, Europhys. Lett. **83**, 67006 (2008).

[4] M. Rotter, M. Tegel, and D. Johrendt, Phys. Rev. Lett. **101**, 107006 (2008).

[5] Y. Su, P. Link, A. Schneidewind, Th. Wolf, P. Adelmann, Y. Xiao, M. Meven, R. Mittal, M. Rotter, D. Johrendt, Th. Brueckel, and M. Loewenhaupt, Phys. Rev. B **79**, 064504 (2009).

[6] Y. Xiao, Y. Su, R. Mittal, T. Chatterji, T. Hansen, C. M. N. Kumar, S. Matsuishi, H. Hosono, and Th. Brueckel, Phys. Rev. B **79**, 060504(R) (2009).

[7] L. Boeri, O. V. Dolgov, and A. A. Golubov, Phys. Rev. Lett. **101**, 026403 (2008).

[8]M. Le Tacon, T. R. Forrest, Ch. Rüegg, A. Bosak, A. C. Walters, R. Mittal, H. M. Rønnow, N. D. Zhigadlo, S. Katrych, J. Karpinski, J. P. Hill, M. Krisch, and D.F. McMorrow, Phys. Rev. B **80**, 220504(R) (2009).

[9]I. I. Mazin, D. J. Singh, M. D. Johannes, and M. H. Du, Phys. Rev. Lett. **101**, 057003 (2008).

[10]K. Kuroki, S. Onari, R. Arita, H. Usui, Y. Tanaka, H. Kontani, and H. Aoki, Phys. Rev. Lett. **101**, 087004 (2008).

[11]T. Bazhirov and M. L. Cohen, Phys. Rev. B **86**, 134517 (2012).

[12]A. Iadecola, B. Joseph, L. Simonelli, A. Puri, Y. Mizuguchi, H. Takeya, Y. Takano, and N. L. Saini, J. Phys. Condens. Matter **24**, 115701 (2012).

[13]W. Bao, Q.-Z. Huang, G.-F. Chen, M. A. Green, D.-M. Wang, J.-B. He, and Y.-M. Qiu, Chin. Phys. Lett. **28**, 086104 (2011).

[14]J. Guo, S. Jin, G. Wang, S. Wang, K. Zhu, T. Zhou, M. He, and X. Chen, Phys. Rev. B **82**, 180520(R) (2010); G. Friemel, W. P. Liu, E. A. Goremychkin, Y. Liu, J. T. Park, O. Sobolev, C. T. Lin, B. Keimer, and D. S. Inosov, Europhys. Lett. **99**, 67004 (2012).

[15]C. H. Li, B. Shen, F. Han, X. Y. Zhu, and H. H. Wen, Phys. Rev. B **83**, 184521 (2011).

[16]A. Krzton-Maziopa, Z. Shermadini, E. Pomjakushina, V. Pomjakushin, M. Bendele, A. Amato, R. Khasanov, H. Luetkens, and K. Conder, J. Phys. Condens. Matter **23**, 052203 (2011).

[17]A. D. Christianson, E. A. Goremychkin, R. Osborn, S. Rosenkranz, M. D. Lumsden, C. D. Malliakas, L. S. Todorov, H. Claus, D. Y. Chung, M. G. Kanatzidis, R. I. Bewley, and T. Guidi, Nature **456**, 930 (2008).

[18]C. de la Cruz, Q. Huang, J. W. Lynn, J. Li, W. Ratcliff II, J. L. Zarestky, H. A. Mook, G. F. Chen, J. L. Luo, N. L. Wang, and P. Dai, Nature **453**, 899 (2008).

[19]W. Bao, Y. Qiu, Q. Huang, M. A. Green, P. Zajdel, M. R. Fitzsimmons, M. Zhernenkov, S. Chang, M. Fang, B. Qian, E. K. Vehstedt, J. Yang, H. M. Pham, L. Spinu, and Z. Q. Mao, Phys. Rev. Lett. **102**, 247001 (2009).

[20]A. M. Zhang, K. Liu, J. H. Xiao, J. B. He, D. M. Wang, G. F. Chen, B. Normand, and Q. M. Zhang, Phys. Rev. B **85**, 024518 (2012).

[21]A. Ignatov, A. Kumar, P. Lubik, R. H. Yuan, W. T. Guo, N. L. Wang, K. Rabe, and G. Blumberg, Phys. Rev. B **86**, 134107 (2012).

[22]C. C. Homes, Z. J. Xu, J. S. Wen, and G. D. Gu, Phys. Rev. B **85**, 180510(R) (2012).

[23]R. Mittal, Y. Su, S. Rols, T. Chatterji, S. L. Chaplot, H. Schober, M. Rotter, D. Johrendt, and Th. Brueckel, Phys. Rev. B **78**, 104514 (2008).

[24]R. Mittal, Y. Su, S. Rols, M. Tegel, S. L. Chaplot, H. Schober, T. Chatterji, D. Johrendt, and Th. Brueckel, Phys. Rev. B **78**, 224518 (2008).

[25]M. Zbiri, R. Mittal, S. Rols, Y. Su, Y. Xiao, H. Schober, S. L. Chaplot, M. R. Johnson, T. Chatterji, Y. Inoue, S. Matsuishi, H. Hosono, and Th. Brueckel, J. Phys. Condens. Matter **22**, 315701 (2010).

[26]R. Mittal, L. Pintschovius, D. Lamago, R. Heid, K.-P. Bohnen, D. Reznik, S. L. Chaplot, Y. Su, N. Kumar, S. K. Dhar, A. Thamizhavel, and Th. Brueckel, Phys. Rev. Lett. **102**, 217001 (2009).

[27]M. Zbiri, H. Schober, M. R. Johnson, S. Rols, R. Mittal, Y. Su, M. Rotter, and D. Johrendt, Phys. Rev. B **79**, 064511 (2009).

[28]T. Yildirim, Phys. Rev. Lett. **102**, 037003 (2009); Phys. C **469**, 425 (2009).

[29]S. Landsgesell, D. Abou-Ras, T. Wolf, D. Alber, and K. Prokes, Phys. Rev. B **86**, 224502 (2012).

[30]D. L. Price and K. Skold, in *Neutron Scattering*, edited by K. Skold and D. L. Price, Vol. A (Academic Press, Orlando, 1986); J. M. Carpenter and D. L. Price, Phys. Rev. Lett. **54**, 441 (1985); S. Rols, H. Jobic, and H. Schober, C. R. de Physique **8**, 777 (2007).

[31]http://www.ncnr.nist.gov; V. F. Sears, Neutron News **3**, 29 (1992); A.-J. Dianoux and G. Lander (Eds.), *Neutron Data Booklet* (Institut Laue-Langevin, Grenoble, France, 2002).

[32]G. Kresse and J. Furthmüller, Comput. Mater. Sci. **6**, 15 (1996).

[33]G. Kresse and D. Joubert, Phys. Rev. B **59**, 1758 (1999).

[34]H. J. Monkhorst and J. D. Pack, Phys. Rev. B **13**, 5188 (1976).

[35]J. P. Perdew, K. Burke, and M. Ernzerhof, Phys. Rev. Lett. **77**, 3865 (1996).

[36]J. P. Perdew, K. Burke, and M. Ernzerhof, Phys. Rev. Lett. **78**, 1396 (1997).

[37]K. Parlinksi, Software phonon (2003).